

1 Conference Proceedings Paper

2 Oxyresveratrol Supplementation In Hyper-Branched 3 Cyclodextrin Based Nanosponges As Antiaging 4 Enhancer in *Caenorhabditis Elegans*

5 Adrián Matencio^{1*}, M. Alejandra Guerrero-Rubio², Fabrizio Caldera¹, Claudio Ceccone¹, Alberto
6 Rubín Pedrazzo¹, Silvia Navarro-Orcajada², Francesco Trotta¹, Francisco García-Carmona² and
7 José Manuel López-Nicolás²

8 ¹ Dip. Di Chimica, Università di Torino, via P. Giuria 7, 10125, Torino, Italy

9 ² Departamento de Bioquímica y Biología Molecular A, Unidad Docente de Biología, Facultad de Veterinaria.
10 Regional Campus of International Excellence "Campus Mare Nostrum". Universidad de Murcia, Murcia,
11 Spain

12 * Correspondence: adrian.matencioduran@unito.it

13 **Abstract:** 1) background: The desire to live longer lives demans novel strategies to perform this
14 target. For that reason, in this work [1] the increase of the *Caenorhabditis elegans* (C.elegans)
15 lifespan extension using hyper-branched cyclodextrin-based nanosponges (CD-NS) complexing
16 oxyresveratrol (OXY) was evaluated. 2) Methods: The titration displacement of fluorescein was
17 used to calculate the apparent complexation constant (K_F) between CD-NS and OXY. Moreover,
18 PDE4 was expressed, purified and refolded in presence of cyclodextrins (CDs) to study its possible
19 inhibition as pharmacological target of OXY. 3) Results: The effect of OXY on PDE4 displayed a
20 competitive *in vitro* inhibition corroborated *in silico*. A maximum increase of the *in vivo* life
21 expectancy of about 9.6% of using OXY/CD-NS complexes in comparison with the control was
22 obtained without toxicity. 4) Conclusions: These results as a whole represent new opportunities to
23 use OXY and CD-NS in lifespan products.

24 **Keywords:** lifespan; *Caenorhabditis elegans*; oxyresveratrol

26 1. Introduction

27 Increasing life expectancy is a common wish for much of humanity. While one of the easiest
28 way to fulfill this wish would be by dietary restriction (DR) [2], a pharmacological approach would
29 be of greater interest to avoid over-strict diets. In this respect, stilbenes have been proposed to act as
30 modulators of the pathway [3]. Stilbenes are a well-known family of bioactive compounds which
31 presents generally several bioactivities such as anticancer, antioxidant, antimicrobial or
32 photoprotective [4].

33 One on the animal models most commonly used for testing drugs in health promoting and
34 anti-aging tests is *Caenorhabditis elegans* (C.elegans) because of its transparent, small size,
35 well-annotated genome, which has many tissues similar to those of animals and a rapid life cycle [5].
36 Its capacity to extend the lifespan depends on sir-2.1/SIRT1-dependent signaling and DAF-16/FOXO
37 thought insulin and IGF-1 signaling (IIS) pathway or oxidative stress protection [6–9]

38 In this respect, one of the enzyme family that regulates this are phosphodiesterases (PDE) [3,10],
39 which comprise a group of enzymes that degrade the phosphodiester bond in the secondary
40 messenger molecules cAMP and cGMP to from AMP and GMP. They regulate the localization,
41 duration, and amplitude of cyclic nucleotide signaling within subcellular domains. PDEs are

42 therefore important regulators of signal transduction mediated by these second messenger
43 molecules.

44 On the other hand, although stilbenes are interesting molecules, its hydrophobicity and low
45 stability [11–14] make their administration difficult. It was therefore thought that using cyclodextrins
46 (CD) and hyper-branched cyclodextrin based nanosponges (CD-NSs) make the administration more
47 stable [15,16]. Indeed, although oxyresveratrol (OXY) has good bioaccessibility [17], insoluble CD-NS
48 has proved the capacity to improve it [18], which would make the administration more effective.

49 CDs are torus-shaped oligosaccharides made up of α -(1,4) linked glucose units, the most
50 common CDs being α , β and γ -CD, which contain six, seven and eight glucose units, respectively,
51 although semisynthetic CDs also exist [19,20]. They present the capacity to complex different
52 molecules creating the commonly called inclusion complex [21,22]. However, when bioactive
53 compounds are to be used as a pharmaceutical product, the release must be slow, and unfortunately,
54 this is not a quality of CD complexes; However, the use of cyclodextrin-based nanosponges, as
55 hyper-branched (CD-NSs) should be also evaluated [23,24]. CD-NSs are cross-linked polymer
56 structures with a three-dimensional network with a crystalline and amorphous structure, spherical
57 in shape and possessing good swelling properties [25].

58 Bearing the above in mind, the work was planned as follows: Firstly, a study of the
59 complexation between OXY and hyper-branched CD-NSs was carried out. Secondly, the in vitro and
60 in silico enzymatic activity of PDE4 and its inhibition by OXY was characterized. Finally, an in vivo
61 lifespan extension of OXY in the presence of CDs and CD-NSs on *C.elegans* were studied.

62 2. Experiments

63 2.1. Materials

64 β -Cyclodextrin (β -CD) was purchased from Roquette (France). Hydroxypropyl-beta- (HP β -CD)
65 was purchased from Carbosynth (Berkshire, UK. DS 5.5). Oxyresveratrol (OXY, CID 5281717) was
66 purchased from TCI Europe and used as received. The remaining chemicals were purchased from
67 Sigma-Aldrich (Madrid, Spain). The samples were stored in darkness

68 2.2. Equipment and Experimental Procedure

69 2.2.1. Preparation of hyper-branched nanosponges

70 Hyper-branched water-soluble β -CD nanosponge was prepared as reported [26]. The white
71 powder was dried and ground in a mortar, obtaining 1.8 g and preserved in darkness and dry
72 conditions.

73 2.2.2. Fluorescein as displacement signal of CD-NS/OXY complex

74 To verify the complexation of Fluorescein by CD-NS, the fluorescence of 25 μ M of fluorescein
75 (ex 494 em 521) was monitored at increasing CD-NS quantities using a Shimadzu RF-6000
76 spectrofluorimeter (Shimadzu, Kyoto, Japan) equipped with thermostatically controlled cells to
77 obtain its fluorescence spectra. Excitation and emission bandwidths were both set at 5 nm. The
78 displacement was carried out studying the effect of increasing OXY (0, 5, 10, 15, 20, 22, 24, 28, 30, 40,
79 50 and 80 μ M) concentration on a 25 μ M of fluorescein mixed with 200 ppm CD-NS. All samples
80 were prepared in water with the exception of fluorescein (acetone). The apparent complexation
81 constant (K_{Fapp}) of OXY/CD-NS was calculated using the equations developed by Selvidge & Eftink
82 in 1986 for CD/ligands interactions [27]. The average molecular weight of CD-NS [26] was used to
83 obtain the concentration of polymer and its apparent complexation constant (K_{Fapp} , here called K_1)
84 with fluorescein using Benesi-Hildebrand plot [28] as intrinsic average constant. After that, the
85 following algebraic solution was applied to obtain the OXY/CD-NS apparent constant (K_{Fapp} , here
86 called K_2):

$$K_2 = \frac{[CD.NS]_0 - \frac{v}{K_1(1-v)} - v[Fluorescein]_0}{\frac{v}{K_1(1-v)}([OXY]_0 - [CD-NS]_0 + v[Fluorescein]_0 + \frac{v}{K_1(1-v)})} \quad (1)$$

88 where [CD-NS]₀, [Fluorescein]₀ and [OXY]₀ are the initial concentration of each molecule and v
89 is the fraction of fluorescein bound to CD-NS (calculated as reported [27]).

90 2.2.3. PDE4 expression, purification and refolding

91 The expression was carried out as reported [29]. After expression, cells were lysed by sonication
92 in 5 pulses of 15 s in a Branson Digital sonifier (Branson Ultrasonic Corporation, Connecticut, USA)
93 and centrifuged at 8000 xg for 30 min at 4°C. The resulting pellet was dissolved in 0.3 M NaCl, 6 M
94 Urea, 1 % Triton X-100, 0.05 M phosphate buffer pH 7.4 with 0.5 mM benzamidine for 30 min at 500
95 rpm and 20 °C in a thermomixer comfort (Eppendorf). It was centrifuged at 8000 xg for 30 min at 4°C
96 and the remaining pellet was dissolved in 0.3 M NaCl, 25 mM ZnSO₄, 2.5 % Triton X-100, 0.05 M
97 phosphate buffer pH 7.4 with 0.5 mM benzamidine for 150 min at 500 rpm and 20 °C in a
98 thermomixer comfort (Eppendorf). The sample was centrifuged at 8000 g for 30 min at 4°C to remove
99 pellet. The supernatant was incubated [30] adding 2 mM β-CD (15 min at 35 °C) and after β-CD until
100 4 mM (15 min at 35 °C). The final solution was concentrated using Amicon Ultra15 50KDa until 100
101 μL. A 10% SDS-PAGE was carried out to check purify and the molecular weight of the final protein
102 with the EZ-Run™ Pre-stained Rec Protein ladder (Fisher). The concentration of PDE4 was
103 determined by the Bradford assay (Biorad) using bovine serum albumin as standard.

104 2.2.4. PDE4 activity assay

105 The assay of PDE4 activity was as previously described [31]. The effect of pH and Mg₂SO₄
106 concentration were studied changing their values in sample buffer. For Km, Vmax and kcat (product
107 generated per enzyme and time) determination, a non-linear plot using Michaelis-Menten kinetic
108 was used.

$$109 \quad V = \frac{V_{max}[S]}{K_m + [S]} = \frac{k_{cat}[E][S]}{K_m + [S]} \quad (2)$$

110 Where [S] is the substrate concentration and [E] the enzyme concentration.

111 For OXY inhibition assay, the I₅₀ (value where the 50% of the enzyme is inhibited) was studied.
112 To obtain K_i (the concentration required to produce half maximum inhibition), a conversion from
113 I₅₀ to K_i for competitive inhibition was applied [32].

$$114 \quad K_i = \frac{I_{50}}{1 + \frac{[S]}{K_m}} \quad (3)$$

115 2.2.5. Molecular modeling and docking

116 The sequence reported by Genscript (deleting 70 aminoacids in N-terminal position) after
117 optimization was uploaded to Swiss-Model [33] with default parameters using PDB ID 4WZI as
118 template. The resulting protein was used to carry out the molecular docking experiments. The model
119 and the ligand (cAMP, RSV or OXY, obtained from ZINC database) were uploaded to Swiss-Dock
120 [34] with default parameters. The results were analyzed using Chimera (Version 1.9) and Pymol
121 (version 1.9).

122 2.2.6. In vivo Lifespan assay in C.elegans

123 The protocol was carried out as reported [35] using lifespan machine [36]. The tested molecules
124 were prepared to achieve the less DMSO possible concentration due to its intrinsic toxicity on
125 C.elegans [37]. Only HPβ-CD samples were possible to use without DMSO. The remaining samples
126 presented 1% DMSO due to OXY solubilization or DMSO remaining in the CD-NS after purification.
127 As control, 1 % DMSO treatment were used in all assays with the exception of HPβ-CD assay. The
128 samples were sterilized by filtration (CD or CD-NS) or autoclave (OXY). All the experiment plates
129 were done in triplicate. The plates were closed and incubated for 20min at 20°C. Plates that present
130 condensation were open under sterile conditions and the lids dried with disposable sterile wipers.

131 Closed lid plates were loaded into the scanners of the lifespan machine. The machine acquired an
132 image of each loaded plate every hour for the duration of the experiment and the analysis detected
133 the time of the death for each worm. The experiments were set at 25°C for 20 days.

134 2.2.7. The OXY apparent critical micellar concentration determination

135 The apparent critical micellar concentration (c.m.c) was carried out as reported [38] with slight
136 modifications. Briefly, tubes with different OXY concentrations (5, 10, 15, 20, 25, 30, 35, 40, 60, 100
137 and 150 μM) using phosphate buffer (pH 6) were incubated in presence of 0.88 μM
138 diphenyl-hexatriene (DPHT) for 10 minutes in darkness. The fluorescence signal (excitation 358,
139 emission 430) of each one was obtained using a Portable Fluorometer Fluo-100 (AllSheng, China)
140 with appropriate filters and compared with the signal of the lowest OXY concentration.

141 2.2.8. Data analysis

142 The experiments were carried out at least in triplicate. Graphical representations and enzymatic
143 kinetic were made using SigmaPlot (Version 10.0). A t-test was applied using social science statistics
144 (<https://www.socscistatistics.com/>) fixing the significance level at $P < 0.05$. Mathematical analysis of
145 the obtained data in Lifespan Machine was performed using the online application for survival
146 analysis OASIS 2 [39] with the Kaplan-Meier estimator, Boschloo's Test, Kolmogorov-Smirnov Test
147 and Survival Time F-Test. Other mathematical operations were carried out using wxMaxima
148 software (version 12.04.0).

149 3. Results and discussion

150 3.1. Fluorescein as a nanosensor for hyper-branched CD-NS complexation and applicable to OXY particles.

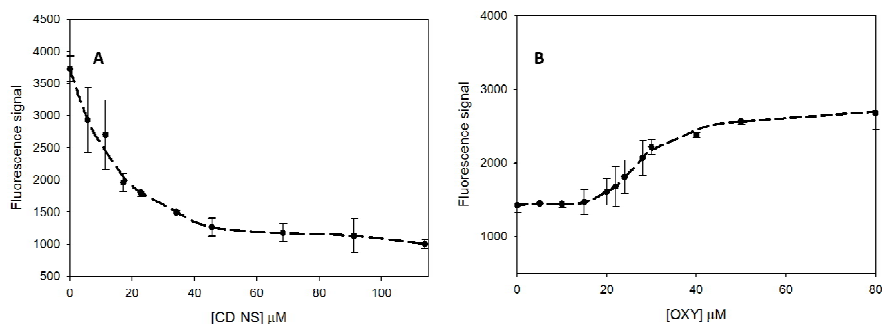
151 The first objective was to demonstrate that hyper-branched CD-NSs could complex OXY. For
152 this, the first tried was to use the intrinsic OXY fluorescence to evaluate K_{Fapp} [40]; however, its low
153 fluorescence signal generated several mistakes. For that reason, a host displacement with fluorescein
154 was used, which is a well-studied CD complexed molecule [41,42]. The complexation of fluorescein
155 quenches the fluorescence signal [41]. The effect of CD-NS on fluorescein is showed in **figure 1A**
156 where it can be seen that the fluorescein signal was decreased by CD-NS addition. No scattering was
157 reported so the data suggest that the decrease in fluorescein signal was due to its complexation. This
158 finding can be used to obtain a K_{Fapp} between fluorescein and CD-NS with a constant " K_1 " of $5.6 \times$
159 $10^4 \pm 2.5 \times 10^3 \text{ M}^{-1}$, $R^2 > 0.99$) using Benesi-Hildebrand plot [28].

160 At this point, the effect of OXY on fluorescein/CD-NS signal was studied to obtain its K_{Fapp} (K_2),
161 using 45.5 μM (200 ppm) of CD-NS to check the K_{F} because it was the concentration where the
162 asymptote started. **Figure 1B** shows that the fluorescein signal increased as a consequence of the
163 entrance of OXY and the release of fluorescein. Using equation 1 at several OXY concentrations [27],
164 the average K_2 value was found at $1.20 \times 10^5 \text{ M}^{-1} \pm 1.23 \times 10^4 \text{ M}^{-1}$. This supports the idea that CD-NS
165 can complex OXY and lays the foundations to evaluate the K_{Fapp} using soluble NS.

166 3.2. *In vitro* and *in silico* PDE4 activity assay and inhibition

167 The next step was to check the activity of the pure refolded PDE4. As the protein was able to
168 convert cAMP to AMP, the optimal pH and $[\text{Mg}^{2+}]$ (the zinc ion is strongly linked to the catalytic
169 center [43,44]) were studied before the enzymatic characterization (data not showed).

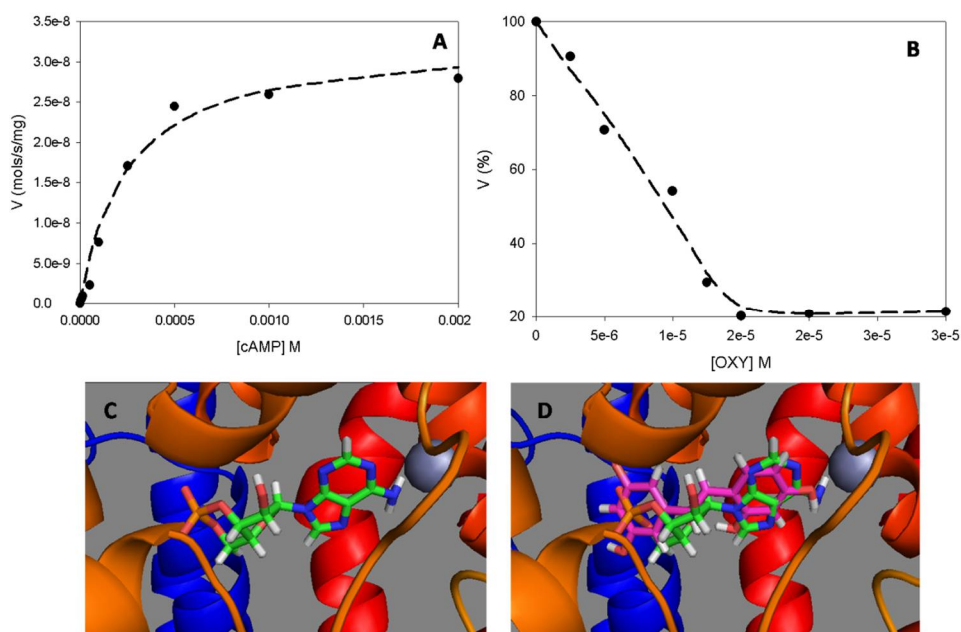
170 **Figure 2A** shows the effect of cAMP on PDE, showing a Michaelis-Menten plot in the optimal
171 conditions (pH 7 and 7.5 mM Mg_2SO_4). The refolded protein gave a $K_{\text{mapp}} = 230 \pm 9 \mu\text{M}$, $V_{\text{maxapp}} = 3.3 \times$
172 $10^{-8} \pm 0.1 \times 10^{-8} \text{ mols/s/mg}$ and $k_{\text{catapp}} = 1 \times 10^{-3} \pm 3 \times 10^{-5} \text{ s}^{-1}$ ($R^2 \approx 0.98$) in a Michaelis Menten plot.



173

174 **Figure 1.** (A) Effect of CD-NS on fluorescein (25 μM) fluorescence signal (conditions: water at 25 °C).
 175 (B) Effect of OXY (0, 5, 10, 15, 20, 22, 24, 28, 30, 40, 50 and 80 μM) concentration on fluorescein/CD-NS
 176 complex fluorescence signal (condition: water at 25 °C).

177 The above data demonstrated that the refolded protein presented activity and perhaps also had
 178 the capacity to test the inhibitory profile against OXY. So, after characterization, the next step was to
 179 study the effect of OXY on the enzymatic activity (**figure 2B**). The $I_{50} = 10 \pm 0.6 \mu\text{M}$ suggests strong
 180 inhibition. Recently, it was reported that human PDE4 presents a resveratrol competitive inhibition
 181 [10]. For that reason, it is reasonable to assume the same inhibition for the protein. The calculation of
 182 K_i was carried out using Eq.3, with a K_{iapp} of $3.2 \pm 0.16 \mu\text{M}$, which pointed to the ability of OXY to
 183 inhibit PDE4 directly *in vitro*, suggesting that this enzyme might be affected after OXY
 184 supplementation.



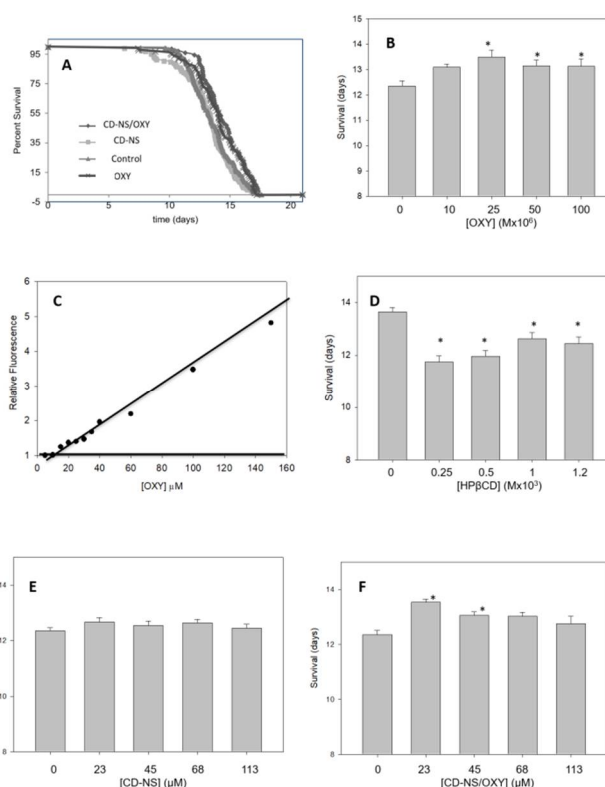
185

186 **Figure 2.** (A) Michaelis-Menten fit of the Effect of cAMP on PDE4 activity (sample buffer at 25 °C). (B)
 187 Effect of OXY on PDE4 activity at 4×10^{-4} M of cAMP (sample buffer at 25 °C). (C) Molecular docking
 188 of cAMP/PDE4, (D) Overlapping OXY and cAMP docking results. (E) Polar interactions of cAMP
 189 with PDE4 and (F) Polar interactions of OXY with PDE4.

190 To check the possibility of non-competitive interactions [45], a molecular docking was carried
 191 out. The molecular modeling of PDE4 also demonstrated that OXY enters the active site of PDE4 to
 192 inhibit the protein (**figure 2C and D**). Moreover, the docking score of cAMP (-8.18) and OXY (-8.56)
 193 would also justify the lower concentration of OXY than cAMP on PDE4.

194 3.5. *In vivo* lifespan on *C.elegans*

195 After demonstrating that PDE4 can be inhibited by OXY (suggesting that this pathway could be
 196 also affected), a lifespan study of the effect of OXY (alone or complexed) on *C.elegans* was carried out
 197 (Figure 3A). The results showed that OXY increases the average life expectancy around 6.5%
 198 ($P < 0.05$) with maximum at 25 μM (Figure 3B). This was interesting, so the low maximum value of
 199 OXY concentration and possible explanations were studied. Our research group has demonstrated
 200 that stilbenes can form aggregates [46] at high concentrations, which may decrease their
 201 bioavailability. To demonstrate this effect on OXY, the apparent critical micellar concentration
 202 (c.m.c) was calculated. The c.m.c of 13 μM obtained suggested the possible aggregation of OXY
 203 (Figure 3C). This would explain the decrease in survival, although it was still better than the control
 204 above 25 μM .



205

206 **Figure 3.** (A) Survival percentage of worms in the presence of 200 ppm CD-NS, 100 μM OXY, and a
 207 mixture of both. (B) Mean lifespan of *C.elegans* in presence of different OXY concentrations. (C)
 208 Effect of OXY on DPHT fluorescence signal. (D) Mean lifespan of *C.elegans* in presence of different
 209 HP β -CD concentrations, (E) Mean lifespan of *C.elegans* in presence of different CD-NS
 210 concentrations. (F) Mean lifespan of *C.elegans* in presence of different CD-NS concentrations at 100
 211 μM OXY (even the control). (* = $P < 0.05$ related to control).

212 To increase OXY disaggregation and stability, its supplementation in the presence of HP- β CD,
 213 one of the least toxic CD derivatives used also to treat the rare disease Niemann Pick type C [47,48],
 214 and hyper-branched CD-NS was considered as a good option. However, HP- β CD was found to be
 215 toxic ($P < 0.05$, figure 3D) for *C.elegans*, the sequestration of essential compounds inside worms such
 216 as membrane cholesterol [49] perhaps affecting their life expectancy. Indeed, there are also known to
 217 be toxic concentrations for human intestine, but its elimination by urine or feces remove them totally
 218 to the system, while plate dishes are close systems preventing this point.

219 On the other hand, hyper-branched CD-NS was not being toxic since its polymeric nature
220 would have a lower uptake capacity for *C.elegans*. Effectively, **figure 3E** showed that the polymer did
221 not present any adverse effect on *C.elegans*. Furthermore, the effect of the polymer on *C.elegans* in
222 presence of OXY increased life expectancy by around 9.6%, which is more than was possible with
223 free OXY (6.5 %, **figure 3F**). The disaggregation effect of CD-NS complexes on OXY and the higher
224 stability would increase the OXY bioavailability [15,24,46]. However, the greater the quantity of
225 CD-NS, the lower effect, perhaps because OXY complexation is much more intense than the quantity
226 released and *C.elegans* cannot use OXY.

227 4. Conclusions

228 In this work synthesized hyper-branched CDs polymers were used to supplement the OXY
229 provided to *C.elegans*. The complexation of OXY by CD-NS was demonstrated by monitoring the
230 displacement of fluorescein. On the other hand, *C.elegans* PDE4 was expressed, refolded and
231 purified. Refolding, with CDs acting as molecular chaperons, was enough to characterize the
232 enzyme activity and its inhibition by OXY, showing its potential role of the regulation of lifespan
233 extension. The inhibition was also studied with molecular docking, showing the most probable
234 interactions between OXY and PDE4. The complex of CD-NS/OXY increased life expectancy more
235 than free OXY. The findings as a whole represent a new opportunity to use OXY as an ingredient of
236 nutraceutical products focused on lifespan extension.

237 **Funding:** This research was funded by the Spanish Ministry of Science and Innovation, project
238 AGL2017-86526-P (MCI/AEI/FEDER, UE), by the “Programa de Ayudas a Grupos de Excelencia de la Región de
239 Murcia, Fundación Séneca, Agencia de Ciencia y Tecnología de la Región de Murcia (Spain)” (Project
240 19893/GERM/15) and by University of Turin research funds (ex 60%).

241 **Acknowledgments:** This work is the result of an aid to postdoctoral training and improvement abroad (for
242 Adrián Matencio) and a predoctoral contract for the training of research staff (for Silvia Navarro-Orcajada)
243 financed by the Consejería de Empleo, Universidades, Empresa y Medio Ambiente of the CARM, through the
244 Fundación Séneca-Agencia de Ciencia y Tecnología de la Región de Murcia.

245 References

- 246 1. Matencio, A.; Guerrero-Rubio, M.A.; Caldera, F.; Cecone, C.; Trotta, F.; García-Carmona, F.;
247 López-Nicolás, J.M. Lifespan extension in *Caenorhabditis elegans* by oxyresveratrol supplementation in
248 hyper-branched cyclodextrin-based nanosponges. *Int. J. Pharm.* **2020**, *589*, 119862,
249 doi:10.1016/j.ijpharm.2020.119862.
- 250 2. Greer, E.L.; Dowlatshahi, D.; Banko, M.R.; Villen, J.; Hoang, K.; Blanchard, D.; Gygi, S.P.; Brunet, A. An
251 AMPK-FOXO pathway mediates longevity induced by a novel method of dietary restriction in *C.*
252 *elegans*. *Curr. Biol. CB* **2007**, *17*, 1646–1656, doi:10.1016/j.cub.2007.08.047.
- 253 3. Reinisalo, M.; Rlund, A.; Koskela, A.; Kaarniranta, K.; Karjalainen, R.O.; Reinisalo, M.;
254 Rlund, A.; Koskela, A.; et al. Polyphenol Stilbenes: Molecular Mechanisms of Defence against Oxidative
255 Stress and Aging-Related Diseases, Polyphenol Stilbenes: Molecular Mechanisms of Defence against
256 Oxidative Stress and Aging-Related Diseases. *Oxidative Med. Cell. Longev. Oxidative Med. Cell. Longev.*
257 **2015**, *2015*, *2015*, doi:10.1155/2015/340520, 10.1155/2015/340520.
- 258 4. El Khawand, T.; Courtois, A.; Valls, J.; Richard, T.; Krisa, S. A review of dietary stilbenes: sources and
259 bioavailability. *Phytochem. Rev.* **2018**, *17*, 1007–1029, doi:10.1007/s11101-018-9578-9.
- 260 5. Corsi, A.K.; Wightman, B.; Chalfie, M. A Transparent Window into Biology: A Primer on *Caenorhabditis*
261 *elegans*. *Genetics* **2015**, *200*, 387–407, doi:10.1534/genetics.115.176099.

- 262 6. Hesp, K.; Smant, G.; Kammenga, J.E. Caenorhabditis elegans DAF-16/FOXO transcription factor and its
 263 mammalian homologs associate with age-related disease. *Exp. Gerontol.* **2015**, *72*, 1–7,
 264 doi:10.1016/j.exger.2015.09.006.
- 265 7. Lee, J.; Kwon, G.; Park, J.; Kim, J.-K.; Lim, Y.-H. Brief Communication: SIR-2.1-dependent lifespan
 266 extension of Caenorhabditis elegans by oxyresveratrol and resveratrol. *Exp. Biol. Med. Maywood NJ* **2016**,
 267 *241*, 1757–1763, doi:10.1177/1535370216650054.
- 268 8. Shen, P.; Yue, Y.; Sun, Q.; Kasireddy, N.; Kim, K.-H.; Park, Y. Piceatannol extends the lifespan of
 269 Caenorhabditis elegans via DAF-16. *BioFactors Oxf. Engl.* **2017**, *43*, 379–387, doi:10.1002/biof.1346.
- 270 9. Sun, X.; Chen, W.-D.; Wang, Y.-D. DAF-16/FOXO Transcription Factor in Aging and Longevity. *Front.*
 271 *Pharmacol.* **2017**, *8*, doi:10.3389/fphar.2017.00548.
- 272 10. Park, S.-J.; Ahmad, F.; Philp, A.; Baar, K.; Williams, T.; Luo, H.; Ke, H.; Rehmann, H.; Taussig, R.; Brown,
 273 A.L.; et al. Resveratrol ameliorates aging-related metabolic phenotypes by inhibiting cAMP
 274 phosphodiesterases. *Cell* **2012**, *148*, 421–433, doi:10.1016/j.cell.2012.01.017.
- 275 11. López-Nicolás, J.M.; García-Carmona, F. Effect of hydroxypropyl- β -cyclodextrin on the aggregation of
 276 (E)-resveratrol in different protonation states of the guest molecule. *Food Chem.* **2010**, *118*, 648–655,
 277 doi:10.1016/j.foodchem.2009.05.039.
- 278 12. Matencio, A.; Hernández-García, S.; García-Carmona, F.; Manuel López-Nicolás, J. An integral study of
 279 cyclodextrins as solubility enhancers of α -methylstilbene, a resveratrol analogue. *Food Funct.* **2017**, *8*, 270–
 280 277, doi:10.1039/C6FO01677D.
- 281 13. Matencio, A.; García-Carmona, F.; López-Nicolás, J.M. Encapsulation of piceatannol, a naturally
 282 occurring hydroxylated analogue of resveratrol, by natural and modified cyclodextrins. *Food Funct.* **2016**,
 283 *7*, 2367–2373, doi:10.1039/c6fo00557h.
- 284 14. Silva, F.; Figueiras, A.; Gallardo, E.; Nerín, C.; Domingues, F.C. Strategies to improve the solubility and
 285 stability of stilbene antioxidants: A comparative study between cyclodextrins and bile acids. *Food Chem.*
 286 **2014**, *145*, 115–125, doi:10.1016/j.foodchem.2013.08.034.
- 287 15. Dhakar, N.K.; Matencio, A.; Caldera, F.; Argenziano, M.; Cavalli, R.; Dianzani, C.; Zanetti, M.;
 288 López-Nicolás, J.M.; Trotta, F. Comparative Evaluation of Solubility, Cytotoxicity and Photostability
 289 Studies of Resveratrol and Oxyresveratrol Loaded Nanosponges. *Pharmaceutics* **2019**, *11*, 545,
 290 doi:10.3390/pharmaceutics11100545.
- 291 16. He, J.; Guo, F.; Lin, L.; Chen, H.; Chen, J.; Cheng, Y.; Zheng, Z.-P. Investigating the oxyresveratrol
 292 β -cyclodextrin and 2-hydroxypropyl- β -cyclodextrin complexes: The effects on oxyresveratrol solution,
 293 stability, and antibrowning ability on fresh grape juice. *LWT* **2019**, *100*, 263–270,
 294 doi:10.1016/j.lwt.2018.10.067.
- 295 17. Chen, W.; Yeo, S.C.M.; Elhennawy, M.G.A.A.; Lin, H.-S. Oxyresveratrol: A bioavailable dietary
 296 polyphenol. *J. Funct. Foods* **2016**, *22*, 122–131, doi:10.1016/j.jff.2016.01.020.
- 297 18. Matencio, A.; Dhakar, N.K.; Bessone, F.; Musso, G.; Cavalli, R.; Dianzani, C.; García-Carmona, F.;
 298 López-Nicolás, J.M.; Trotta, F. Study of oxyresveratrol complexes with insoluble cyclodextrin based
 299 nanosponges: Developing a novel way to obtain their complexation constants and application in an
 300 anticancer study. *Carbohydr. Polym.* **2020**, *231*, 115763, doi:10.1016/j.carbpol.2019.115763.
- 301 19. Kurkov, S.V.; Loftsson, T. Cyclodextrins. *Int. J. Pharm.* **2013**, *453*, 167–180,
 302 doi:10.1016/j.ijpharm.2012.06.055.
- 303 20. Matencio, A.; Navarro-Orcajada, S.; García-Carmona, F.; López-Nicolás, J.M. Applications of
 304 cyclodextrins in food science. A review. *Trends Food Sci. Technol.* **2020**, doi:10.1016/j.tifs.2020.08.009.

- 305 21. Jansook, P.; Ogawa, N.; Loftsson, T. Cyclodextrins: structure, physicochemical properties and
 306 pharmaceutical applications. *Int. J. Pharm.* **2018**, *535*, 272–284, doi:10.1016/j.ijpharm.2017.11.018.
- 307 22. Matencio, A.; Navarro-Orcajada, S.; García-Carmona, F.; Manuel López-Nicolás, J. Ellagic acid–borax
 308 fluorescence interaction: application for novel cyclodextrin-borax nanosensors for analyzing ellagic acid
 309 in food samples. *Food Funct.* **2018**, *9*, 3683–3687, doi:10.1039/C8FO00906F.
- 310 23. Hirayama, F.; Uekama, K. Cyclodextrin-based controlled drug release system. *Adv. Drug Deliv. Rev.* **1999**,
 311 *36*, 125–141, doi:10.1016/S0169-409X(98)00058-1.
- 312 24. Sherje, A.P.; Dravyakar, B.R.; Kadam, D.; Jadhav, M. Cyclodextrin-based nanosponges: A critical review.
 313 *Carbohydr. Polym.* **2017**, *173*, 37–49, doi:10.1016/j.carbpol.2017.05.086.
- 314 25. Cavalli, R.; Trotta, F.; Tumiatti, W. Cyclodextrin-based Nanosponges for Drug Delivery. *J. Incl. Phenom.*
 315 *Macrocycl. Chem.* **2006**, *56*, 209–213, doi:10.1007/s10847-006-9085-2.
- 316 26. Trotta, F.; Caldera, F.; Cavalli, R.; Mele, A.; Punta, C.; Melone, L.; Castiglione, F.; Rossi, B.; Ferro, M.;
 317 Crupi, V.; et al. Synthesis and characterization of a hyper-branched water-soluble β -cyclodextrin
 318 polymer. *Beilstein J. Org. Chem.* **2014**, *10*, 2586–2593, doi:10.3762/bjoc.10.271.
- 319 27. Selvidge, L.A.; Eftink, M.R. Spectral displacement techniques for studying the binding of
 320 spectroscopically transparent ligands to cyclodextrins. *Anal. Biochem.* **1986**, *154*, 400–408,
 321 doi:10.1016/0003-2697(86)90005-9.
- 322 28. Benesi, H.A.; Hildebrand, J.H. A Spectrophotometric Investigation of the Interaction of Iodine with
 323 Aromatic Hydrocarbons. *J. Am. Chem. Soc.* **1949**, *71*, 2703–2707, doi:10.1021/ja01176a030.
- 324 29. Matencio, A.; García-Carmona, F.; López-Nicolás, J.M. Characterization of Resveratrol, Oxyresveratrol,
 325 Piceatannol and Roflumilast as Modulators of Phosphodiesterase Activity. Study of Yeast Lifespan.
 326 *Pharmaceutics* **2020**, *13*, 225, doi:10.3390/ph13090225.
- 327 30. Rozema, D.; Gellman, S.H. Artificial chaperone-assisted refolding of carbonic anhydrase B. *J. Biol. Chem.*
 328 **1996**, *271*, 3478–3487.
- 329 31. Matencio, A.; García-Carmona, F.; López-Nicolás, J.M. An improved “ion pairing agent free” HPLC-RP
 330 method for testing cAMP Phosphodiesterase activity. *Talanta* **2019**, *192*, 314–316,
 331 doi:10.1016/j.talanta.2018.09.058.
- 332 32. Yung-Chi, C.; Prusoff, W.H. Relationship between the inhibition constant (KI) and the concentration of
 333 inhibitor which causes 50 per cent inhibition (I50) of an enzymatic reaction. *Biochem. Pharmacol.* **1973**, *22*,
 334 3099–3108, doi:10.1016/0006-2952(73)90196-2.
- 335 33. Waterhouse, A.; Bertoni, M.; Bienert, S.; Studer, G.; Tauriello, G.; Gumienny, R.; Heer, F.T.; de Beer,
 336 T.A.P.; Rempfer, C.; Bordoli, L.; et al. SWISS-MODEL: homology modelling of protein structures and
 337 complexes. *Nucleic Acids Res.* **2018**, *46*, W296–W303, doi:10.1093/nar/gky427.
- 338 34. Grosdidier, A.; Zoete, V.; Michielin, O. SwissDock, a protein-small molecule docking web service based
 339 on EADock DSS. *Nucleic Acids Res.* **2011**, *39*, W270-277, doi:10.1093/nar/gkr366.
- 340 35. Guerrero-Rubio, M.A.; Hernández-García, S.; García-Carmona, F.; Gandía-Herrero, F. Extension of
 341 life-span using a RNAi model and in vivo antioxidant effect of Opuntia fruit extracts and pure betalains
 342 in *Caenorhabditis elegans*. *Food Chem.* **2019**, *274*, 840–847, doi:10.1016/j.foodchem.2018.09.067.
- 343 36. Stroustrup, N.; Ulmschneider, B.E.; Nash, Z.M.; López-Moyado, I.F.; Apfeld, J.; Fontana, W. The
 344 *Caenorhabditis elegans* Lifespan Machine. *Nat. Methods* **2013**, *10*, 665–670, doi:10.1038/nmeth.2475.
- 345 37. Hart, A. Behavior. *WormBook* **2006**, doi:10.1895/wormbook.1.87.1.

- 346 38. Matencio, A.; García-Carmona, F.; López-Nicolás, J.M. Aggregation of t10,c12 conjugated linoleic Acid in
 347 presence of natural and modified cyclodextrins. A physicochemical, thermal and computational analysis.
 348 *Chem. Phys. Lipids* **2017**, *204*, 57–64, doi:10.1016/j.chemphyslip.2017.03.008.
- 349 39. Han, S.K.; Lee, D.; Lee, H.; Kim, D.; Son, H.G.; Yang, J.-S.; Lee, S.-J.V.; Kim, S. OASIS 2: online application
 350 for survival analysis 2 with features for the analysis of maximal lifespan and healthspan in aging
 351 research. *Oncotarget* **2016**, *7*, 56147–56152, doi:10.18632/oncotarget.11269.
- 352 40. Matencio, A.; García-Carmona, F.; López-Nicolás, J.M. The inclusion complex of oxyresveratrol in
 353 modified cyclodextrins: A thermodynamic, structural, physicochemical, fluorescent and computational
 354 study. *Food Chem.* **2017**, *232*, 177–184, doi:10.1016/j.foodchem.2017.04.027.
- 355 41. Politzer, I.R.; Crago, K.T.; Hampton, T.; Joseph, J.; Boyer, J.H.; Shah, M. Effect of β -cyclodextrin on the
 356 fluorescence, absorption and lasing of rhodamine 6G, rhodamine B and fluorescein disodium salt in
 357 aqueous solutions. *Chem. Phys. Lett.* **1989**, *159*, 258–262, doi:10.1016/0009-2614(89)87420-2.
- 358 42. Flamigni, L. Inclusion of fluorescein and halogenated derivatives in .alpha.-, .beta.-, and
 359 .gamma.-cyclodextrins: a steady-state and picosecond time-resolved study. *J. Phys. Chem.* **1993**, *97*, 9566–
 360 9572, doi:10.1021/j100140a006.
- 361 43. Suoranta, K.; Londesborough, J. Purification of intact and nicked forms of a zinc-containing,
 362 Mg²⁺-dependent, low Km cyclic AMP phosphodiesterase from bakers' yeast. *J. Biol. Chem.* **1984**, *259*,
 363 6964–6971.
- 364 44. Xiong, Y.; Lu, H.-T.; Li, Y.; Yang, G.-F.; Zhan, C.-G. Characterization of a Catalytic Ligand Bridging Metal
 365 Ions in Phosphodiesterases 4 and 5 by Molecular Dynamics Simulations and Hybrid Quantum
 366 Mechanical/Molecular Mechanical Calculations. *Biophys. J.* **2006**, *91*, 1858–1867,
 367 doi:10.1529/biophysj.106.086835.
- 368 45. Martínez-Moñino, A.B.; Zapata-Pérez, R.; García-Saura, A.G.; Gil-Ortiz, F.; Pérez-Gilabert, M.;
 369 Sánchez-Ferrer, Á. Characterization and mutational analysis of a nicotinamide mononucleotide
 370 deamidase from *Agrobacterium tumefaciens* showing high thermal stability and catalytic efficiency.
 371 *PLOS ONE* **2017**, *12*, e0174759, doi:10.1371/journal.pone.0174759.
- 372 46. López-Nicolás, J.M.; García-Carmona, F. Aggregation state and pKa values of (E)-resveratrol as
 373 determined by fluorescence spectroscopy and UV-visible absorption. *J. Agric. Food Chem.* **2008**, *56*, 7600–
 374 7605, doi:10.1021/jf800843e.
- 375 47. Gould, S.; Scott, R.C. 2-Hydroxypropyl- β -cyclodextrin (HP- β -CD): A toxicology review. *Food Chem.*
 376 *Toxicol.* **2005**, *43*, 1451–1459, doi:10.1016/j.fct.2005.03.007.
- 377 48. Matencio, A.; Navarro-Orcajada, S.; González-Ramón, A.; García-Carmona, F.; López-Nicolás, J.M.
 378 Recent advances in the treatment of Niemann pick disease type C: A mini-review. *Int. J. Pharm.* **2020**, *584*,
 379 119440, doi:10.1016/j.ijpharm.2020.119440.
- 380 49. Castagne, D.; Fillet, M.; Delattre, L.; Evrard, B.; Nusgens, B.; Piel, G. Study of the cholesterol extraction
 381 capacity of β -cyclodextrin and its derivatives, relationships with their effects on endothelial cell viability
 382 and on membrane models. *J. Incl. Phenom. Macrocycl. Chem.* **2008**, *63*, 225–231,
 383 doi:10.1007/s10847-008-9510-9.

384 **Publisher's Note:** MDPI stays neutral with regard to jurisdictional claims in published maps and institutional
 385 affiliations.



© 2020 by the authors; licensee MDPI, Basel, Switzerland. This article is an open access article distributed under the terms and conditions of the Creative Commons by

